

# Numerical renormalization-group study of spin correlations in one-dimensional random spin chains

T. Hikihara

*Graduate School of Science and Technology, Kobe University, Rokkodai, Kobe 657-8501, Japan*

A. Furusaki and M. Sigrist

*Yukawa Institute for Theoretical Physics, Kyoto University, Sakyo-ku, Kyoto 606-8502, Japan*

(May 10, 2018)

We calculate the ground-state two-spin correlation functions of spin- $\frac{1}{2}$  quantum Heisenberg chains with random exchange couplings using the real-space renormalization group scheme. We extend the conventional scheme to take account of the contribution of local higher multiplet excitations in each decimation step. This extended scheme can provide highly accurate numerical data for large systems. The random average of staggered spin correlations of the chains with random antiferromagnetic (AF) couplings shows algebraic decay like  $1/r^2$ , which verifies the Fisher's analytic results. For chains with random ferromagnetic (FM) and AF couplings, the random average of generalized staggered correlations is found to decay more slowly than a power-law, in the form close to  $1/\ln(r)$ . The difference between the distribution functions of the spin correlations of the random AF chains and of the random FM-AF chains is also discussed.

## I. INTRODUCTION

One-dimensional (1D) quantum spin systems have attracted much attention over the decades. This is not only because these systems have been a good testing ground for various theoretical techniques and approximations but also because they exhibit a wealth of fascinating phenomena in their ground states and low-lying excitations. These include quasi long-range-order (LRO), topological order and ground-state phase transitions, which are all purely quantum effects due to the low-dimensionality of the systems. Among these quantum phenomena, the effects of randomness on quantum spin systems have been studied intensively by many groups. These studies revealed the appearance of various exotic phases, which are realized neither in regular quantum systems nor classical random systems. The interplay of randomness and quantum fluctuations plays an essential role in these phases. Systems which are gapless in the absence of randomness are unstable against weak randomness,<sup>1,2</sup> while gapped systems, e.g. integer spin chains in the Haldane phase and dimerized chains, are comparatively robust.<sup>3-5</sup>

A simplest model of the 1D random spin- $\frac{1}{2}$  Heisenberg spin systems is described by the Hamiltonian of the form

$$H = \sum_{i=1}^{L-1} J_i \vec{s}_i \cdot \vec{s}_{i+1}, \quad (1)$$

where  $\vec{s}_i$  are  $S = \frac{1}{2}$  spin operators and the exchange coupling constants  $J_i$  are distributed randomly according to a probability distribution  $P(J_i)$ . There are several quasi-1D systems which provide the realizations of the model Hamiltonian (1). To our knowledge, the first example of such systems belongs to the class of the organic charge-transfer salts tetracyanoquinodimethanide (TCNQ).<sup>6</sup> The low-temperature magnetic properties of these systems are successfully described by the model Hamiltonian (1) with random antiferromagnetic (AF) coupling,<sup>7</sup> in which the couplings  $J_i$  are restricted to take positive random values. A more recently studied system<sup>8</sup> is  $\text{Sr}_3\text{CuPt}_{1-x}\text{Ir}_x\text{O}_6$ . While the pure compounds  $\text{Sr}_3\text{CuPtO}_6$  and  $\text{Sr}_3\text{CuIrO}_6$  represent, respectively, AF and ferromagnetic (FM) spin chains,  $\text{Sr}_3\text{CuPt}_{1-x}\text{Ir}_x\text{O}_6$  contains both AF and FM couplings. The fraction of FM bonds is simply related to the concentration  $x$  of Ir. These compounds are modeled adequately by the Hamiltonian (1) with  $P(J_i) = p\delta(J_i + J) + (1-p)\delta(J_i - J)$ , where  $p$  is the probability of FM bonds. The experimental data of the susceptibility of the compounds were in fact explained successfully by a theory based on the Hamiltonian (1) with the above probability distribution of FM and AF bonds.<sup>9</sup> The model (1) is also realized in the low-temperature regime of randomly depleted 1D spin- $\frac{1}{2}$  even-leg ladders.<sup>10</sup> In these systems, effective  $S = \frac{1}{2}$  spins are induced in the vicinity of each depleted site.<sup>11-17</sup> If the density of depleted spins is sufficiently small, the induced effective spins are the only degrees of freedom which are active in the low-energy limit. The strength of the residual interaction between effective spins depends on the distance between the effective spins, and the coupling can be either antiferromagnetic or ferromagnetic, depending

on whether or not two spins are depleted from the same sublattice. Thus, the low-energy physics of the randomly depleted spin- $\frac{1}{2}$  even-leg ladders is described as a random spin chain with both AF and FM exchange couplings.<sup>13</sup>

For 1D random spin chains containing only AF couplings, rather complete theoretical understanding on their low-energy properties has been achieved. One of the most powerful techniques to study such systems is the real-space renormalization group (RSRG) method introduced by Ma, Dasgupta, and Hu.<sup>1</sup> The basic idea of this method is iterative decimation of spin degrees of freedom by integrating out the strongest bonds in the chain successively. For the random AF chains this procedure keeps the form of the Hamiltonian (1) and renormalizes the probability distribution  $P(J_i)$ . Fisher has given a solution to this RG equation of  $P(J_i)$  that becomes exact in the low-energy limit and shown that any normalizable initial distribution  $P(J_i)$  flows to a single universal fixed point distribution.<sup>2</sup> The ground state of the chain which belongs to the fixed point is characterized by the “random singlet phase,” where each spin forms a singlet with another spin which can be arbitrarily far away. From the intuitive picture of the random singlet phase, Fisher has also shown that the random average of the two-spin correlation function in this phase decays algebraically like  $1/r^2$  with  $r$  being the distance between the two spins. The main contribution to the average comes from the rare events that two spins separated by the distance  $r$  form a singlet pair. The  $1/r^2$  power-law decay has been verified by a numerical calculation for the random  $XX$  spin- $\frac{1}{2}$  chains,<sup>18</sup> which can be mapped to a disordered system of noninteracting fermions.

The random spin chains containing both AF and FM couplings have also been studied theoretically for the last five years, from which a qualitative picture of the low-energy physics of such random FM-AF chains has emerged. Westerberg *et al.*<sup>19</sup> have adapted the RSRG scheme and shown through extensive numerical simulations that the distribution  $P(J_i)$  is renormalized to a single universal fixed-point distribution unless the initial distribution is highly singular around  $J_i = 0$ . The chain at this fixed point can be viewed as an ensemble of weakly interacting large effective spins whose average size  $\bar{S} \propto T^{-\kappa}$  with  $\kappa \approx 0.22$  for temperature  $T \rightarrow 0$ . These large effective spins are generated as a result of decimations of two spins coupled via a strong FM coupling into a larger spin. The results of the RSRG simulations are supported by a recent calculation by Frischmuth *et al.*,<sup>20</sup> who have used the continuous-time quantum Monte Carlo loop algorithm. In contrast to the success in the quantitative calculations on the thermodynamic properties, less is known about the spin correlations in the random FM-AF chains. Since the average size of the effective spins becomes very large in the low-energy (long-distance) limit, one can expect that the system should be close to a classical spin chain that can show the LRO of the generalized staggered spin component. One might also argue, however, that there should be no LRO in 1D quantum spin chains. It is therefore an interesting open question how the correlation function of the generalized staggered moment (whose definition will be given in Sec. III) behaves in the ground state. The purpose of this paper is in fact to present results of our extensive numerical calculation of the two-spin correlation function. We find that it decays very slowly with the form close to  $1/\ln(r)$ , which is consistent with the naive argument that the ground state is extremely long-range correlated, but not really long-range ordered.

The outline of this paper is as follows. Section II A is devoted to a brief review of the RSRG scheme of the generalized version which is applicable to both random AF and FM-AF case. Using the Wigner-Eckart theorem,<sup>21</sup> we simplify the algorithm to allow for calculating the two-spin correlation function between original  $S = \frac{1}{2}$  spins. In section II B, in order to achieve higher accuracy, we extended the RSRG scheme to take into account the contributions of local excitations to the ground state of the whole system. We perform these conventional and extended RSRG algorithm numerically on both random AF and FM-AF chains to calculate the “staggered” spin correlations on their ground states. The results on the random AF case are shown in section III A. In section III B, we show the results on the random FM-AF case. Analyzing the data obtained with the extended RSRG method (which can be applied to larger systems than the DMRG), we conclude that the mean correlations on the random FM-AF case decay very slowly with logarithmic dependence on  $r$ . We also discuss the distribution functions of the logarithm of the correlation functions in section III C. We find that, in the random AF case, the rare spin pairs, which are strongly correlated, dominate the mean correlation while such rare events are not essential in the random FM-AF case. Finally, our results are summarized in section IV.

## II. THE RSRG ALGORITHM

Ma, Dasgupta and Hu introduced a RSRG procedure to investigate the low-temperature properties of random AF spin chains.<sup>1</sup> The method has been generalized to the random FM-AF case by Westerberg *et al.*<sup>19</sup> In this section we explain our extension of this scheme to calculate the ground-state two-spin correlation functions. We begin with a brief review of the RSRG method for the random FM-AF case.

## A. Conventional RSRG

Let us consider a random FM-AF spin- $\frac{1}{2}$  chain described by the Hamiltonian (1). The basic strategy of RSRG is to decimate spin degrees of freedom by combining two spins connected via a strong bond into one effective spin. Consequently, the system is described in terms of effective spins of various sizes coupled by random exchange interactions, although the original Hamiltonian (1) consists of only  $S = 1/2$  spins. We accordingly treat the effective Hamiltonian,

$$H = \sum_l J_l \vec{S}_l \cdot \vec{S}_{l+1}, \quad (2)$$

where both the coupling  $J_l$  and the size of the effective spins  $S_l$  are random. We call the  $S = 1/2$  spins  $\vec{s}_i$  appearing in the Hamiltonian (1) “original” spins in the following to distinguish them from the effective spins  $\vec{S}_l$ .

We define  $\Delta_l$  as the energy gap between the ground-state multiplet and the first excited multiplet of the corresponding bond Hamiltonian  $H_l = J_l \vec{S}_l \cdot \vec{S}_{l+1}$ ,

$$\Delta_l = \begin{cases} |J_l|(S_l + S_{l+1}) & (J_l < 0) \\ J_l(|S_l - S_{l+1}| + 1) & (J_l > 0) \end{cases}$$

and focus on the bond with the largest gap  $\Delta_l$  in the chain. The terms in the effective Hamiltonian (2) which involve the effective spins  $\vec{S}_l$  and  $\vec{S}_{l+1}$  are

$$H' = H'_0 + H'_1 \quad (3)$$

where

$$H'_0 = J_l \vec{S}_l \cdot \vec{S}_{l+1}, \quad (4)$$

$$H'_1 = J_{l-1} \vec{S}_{l-1} \cdot \vec{S}_l + J_{l+1} \vec{S}_{l+1} \cdot \vec{S}_{l+2}. \quad (5)$$

If  $\Delta_l$  is much larger than the gaps of the neighboring bonds,  $\Delta_{l-1}$  and  $\Delta_{l+1}$ , the spins  $\vec{S}_l$  and  $\vec{S}_{l+1}$ , to a good approximation, are frozen into the ground-state multiplet of the local Hamiltonian  $H'_0$ . We, therefore, replace the block composed of  $\vec{S}_l$  and  $\vec{S}_{l+1}$  by the single effective spin  $\vec{S}$ . The Wigner-Eckart theorem<sup>21</sup> then implies that both  $\vec{S}_l$  and  $\vec{S}_{l+1}$  are proportional to  $\vec{S}$ :

$$\begin{aligned} \vec{S}_l &= \alpha \vec{S}, \\ \vec{S}_{l+1} &= \beta \vec{S}, \end{aligned} \quad (6)$$

where  $\alpha$  and  $\beta$  can be obtained from the Clebsch-Gordan coefficients. Substituting Eq. (6) into the four-spin Hamiltonian (3), we obtain, apart from a constant term coming from  $H'_0$ ,

$$\tilde{H} = \tilde{J}_{l-1} \vec{S}_{l-1} \cdot \vec{S} + \tilde{J}_{l+1} \vec{S} \cdot \vec{S}_{l+2}, \quad (7)$$

where

$$\begin{aligned} \tilde{J}_{l-1} &= \alpha J_{l-1}, \\ \tilde{J}_{l+1} &= \beta J_{l+1}. \end{aligned}$$

The case where  $J_l$  is antiferromagnetic with  $S_l = S_{l+1}$  needs a special treatment. In this case the two spins  $\vec{S}_l$  and  $\vec{S}_{l+1}$  form a singlet, and accordingly, we remove both spins from the effective Hamiltonian. Between the spins  $\vec{S}_{l-1}$  and  $\vec{S}_{l+2}$ , a coupling is generated through a second-order process that virtually breaks the singlet of  $\vec{S}_l$  and  $\vec{S}_{l+1}$ . We obtain

$$\tilde{H} = \tilde{J} \vec{S}_{l-1} \cdot \vec{S}_{l+2}, \quad (8)$$

where

$$\tilde{J} = \frac{2J_{l-1}J_{l+1}}{3J_l} S_l(S_l + 1).$$

By replacing the four-spin Hamiltonian (3) with  $\tilde{H}$  [Eq. (7) or Eq. (8)] in the Hamiltonian of the whole system, we obtain a new effective Hamiltonian (See Fig. 1). We note that this procedure preserves the form of the effective Hamiltonian (2) but changes the distributions of the exchange couplings,  $J_l$ , and the size of effective spins,  $S_l$ . We repeat this procedure of integrating out the strongest bonds in a chain successively until the distribution functions for  $J_l$  and  $S_l$  converge to a scaling form. This RG flow has been investigated extensively for various initial distributions including both AF and FM-AF case.<sup>1,19</sup> In particular, for the random AF  $S = 1/2$  chains Fisher has solved the RG equation exactly.<sup>2</sup>

It is also possible to calculate the correlation functions between original spins within the scheme described above. Here we make use of the fact that the original spin operator  $\vec{s}_i$  is, at every step in the RSRG procedure, proportional to the effective spin  $\vec{S}_l$  to which it belongs. We can keep track of the coefficient for each original spin operator by applying Eq. (6) at each step. At the step where the effective spins  $\vec{S}_l$  and  $\vec{S}_{l+1}$  is added into  $\vec{S}$ , we calculate the correlations between  $\vec{s}_i$  and  $\vec{s}_j$  in the ground state of the bond Hamiltonian  $H'_0$ ,

$$\langle \vec{s}_i \cdot \vec{s}_j \rangle = \alpha_i \alpha_j \langle \vec{S}_l \cdot \vec{S}_{l+1} \rangle, \quad (9)$$

where  $\langle \dots \rangle$  represents the expectation value in the ground state;  $\vec{s}_i$  and  $\vec{s}_j$  belong to  $\vec{S}_l$  and  $\vec{S}_{l+1}$ , respectively;  $\alpha_i$  and  $\alpha_j$  are the proportionality coefficients for each spin.

## B. Extension of the RSRG scheme

As seen in the previous subsection, the conventional RSRG procedure consists of “diagonalizing the bond Hamiltonian with the largest gap” and “projecting the low-energy states onto the lowest multiplet.” This means that we completely neglect the contribution of the excited multiplets of the local Hamiltonian (4) to the ground state of the whole system. This approximation is valid only if the energy gap of  $H'_0$  is much larger than the ones of the neighboring bonds. Fisher’s solution for the random AF  $S = 1/2$  chain becomes asymptotically exact since this condition is satisfied near the fixed point of the RG flow.

However, the condition is often not satisfied, in particular, in the early stage of the RG, unless the initial distribution of energy gap is very broad. As a result, we have no choice but to cut off the contributions of local excitations. This is a poor approximation that has a serious effect especially on the calculation of the expectation values of microscopic operators such as the original spins. The ground-state correlation functions between original spins calculated via the conventional RSRG in fact deviate largely from those obtained from the DMRG method and the extended RSRG algorithm described below (See Fig. 3 and Fig. 5 in section III).

One possible prescription to avoid this error is “to keep the local multiplet excitations” at each step. Of course, if we keep all eigenstates of the bond Hamiltonian  $H'_0$  at every step of the RG, the calculation on  $H'_0$  in the final step is equivalent to the exact diagonalization on the Hamiltonian of the whole system. In practice what we should do is to extend the RSRG algorithm under the policy that we keep as many states as we can store in computer memories. In the original RSRG scheme a segment of original spins are combined and represented by a single effective spin. In the extended scheme we keep more states than the lowest multiplet and call the segment a ‘block.’ Each block consists of several original spins and is represented by ‘block states,’ which are the  $m$ -lowest eigenstates of the block Hamiltonian. Since we have to keep or discard all states of a multiplet to ensure the SU(2) symmetry, the actual number of kept states for block  $l$  is  $m_l^* \leq m$ . An original spin operator in block  $l$  is represented by  $m_l^* \times m_l^*$  matrix on the set of the block states accordingly.

Let us consider the effective Hamiltonian

$$H = \sum_l H_l^{(B)} + \sum_l H_{l,l+1} \quad (10)$$

$$H_{l,l+1} = \tilde{J}_l \vec{s}_l^{(R)} \cdot \vec{s}_{l+1}^{(L)}, \quad (11)$$

where  $H_l^{(B)}$  is a block Hamiltonian of the  $l$ th block, diagonal in the block states;  $H_{l,l+1}$  is a coupling Hamiltonian between the  $l$ th and  $(l+1)$ th blocks;  $\vec{s}_l^{(R)}$  and  $\vec{s}_l^{(L)}$  are original spin operators on the right and left edge of the  $l$ th block, respectively;  $\tilde{J}_l$  is a coupling between  $\vec{s}_l^{(R)}$  and  $\vec{s}_{l+1}^{(L)}$ . In the extended RSRG scheme we renormalize the two-block Hamiltonian

$$H'_{l,l+1} = H_l^{(B)} + H_{l,l+1} + H_{l+1}^{(B)} \quad (12)$$

with the largest gap  $\Delta_l$  into one block Hamiltonian (see Fig. 2). Here we define  $\Delta_l$  as the energy difference between the highest energy in the eigen-multiplets of  $H'_{l,l+1}$  which will be kept and the lowest energy in the multiplets which

will be discarded after the decimation. The basic scheme of the extended RSRG is the same as the conventional RSRG except the changes described above. The algorithm is summarized as follows:

- (i) Focus on the bond with the largest gap  $\Delta_l$ . Construct the two-block Hamiltonian (12) of the bond.
- (ii) Diagonalize the two-block Hamiltonian to find a set of eigenvalues and eigenstates. At this point, we can calculate expectation values of various operators in the two blocks, such as the two-spin correlation functions between the original spins, using the ground state of the two-block Hamiltonian.
- (iii) Discard all but the lowest  $m_l^* (\leq m)$  eigenstates in the block Hamiltonian.
- (iv) Express operators, such as the block Hamiltonian itself and the original spin operators in the new block, in terms of the new block states.
- (v) Rewrite the coupling Hamiltonians between the new block and its neighboring blocks in terms of the new  $\vec{s}^{(L)}$  and  $\vec{s}^{(R)}$ . Diagonalize them to update the distribution of the energy gap  $\Delta$ .
- (vi) Return to the step (i).

We obtain all two-spin correlation functions by repeating this procedure until the whole chain is finally represented by one block.

### III. NUMERICAL RESULTS

Using both the conventional RSRG and the extended RSRG with various values of  $m$ , we calculated the correlation functions  $\langle \vec{s}_i \cdot \vec{s}_j \rangle$  in the ground state of open chains for both the random AF case and the random FM-AF case. The maximum size of the chains used for the conventional and the extended RSRG simulations is  $L = 100000$  and  $L = 1000$ , respectively. In the FM-AF case, the random average of the spin correlation,  $\langle \vec{s}_i \cdot \vec{s}_j \rangle$ , always decays exponentially<sup>19</sup> and is not an appropriate quantity to characterize the spin correlation because the sign of  $\langle \vec{s}_i \cdot \vec{s}_j \rangle$  can be either positive or negative depending on the number of AF bonds between  $\vec{s}_i$  and  $\vec{s}_j$ . Instead we introduce the “generalized staggered” correlation function

$$C(|i - j|) = \eta_{ij} \langle \vec{s}_i \cdot \vec{s}_j \rangle, \quad (13)$$

where  $\eta_{ij} = \prod_{k=i}^{j-1} \text{sgn}(-J_k)$  for  $j > i$ . For random AF case,  $C(r)$  is the usual staggered spin correlation. We take the random average of  $C(r)$  and  $\ln C(r)$ , which represents the mean correlations and the logarithm of the typical correlations, respectively. Note that it is impossible to take the random average of  $\ln C(r)$  numerically in the conventional RSRG algorithm, within which  $C(r) = 0$  for two spins that do not form a singlet pair. To check the results of the RSRG methods, we also calculated the correlation functions on  $L = 100$  open chains using the DMRG method<sup>22</sup> with the improved algorithm proposed by White.<sup>23</sup> The number of kept states in the DMRG calculation was up to 100 and 200 for the random AF and FM-AF case, respectively. In both cases, the mean and typical correlations calculated by the extended RSRG are in excellent agreement with those by DMRG (see below). We note that the systems we have treated are much bigger than those in the earlier work by Hida,<sup>24</sup> in which the DMRG method is applied for the FM-AF chains.

#### A. Random AF case

As a typical probability distribution of the random AF case, we choose the box-type bond distribution  $P(J_i)$ ,

$$P(J_i) = \begin{cases} \frac{1}{J_0} & (0 \leq J_i \leq J_0) \\ 0 & (\text{otherwise}) \end{cases} \quad (14)$$

where the cutoff,  $J_0$ , is taken as energy unit. For the random AF case, it is known that any normalizable initial distribution flows to a single universal fixed point.<sup>2</sup> Hence, the results we obtained for the initial distribution (14) are generic. The number of sample chains we used for each method are shown in Table I.

Before discussing our numerical results, we briefly comment on the  $m$ -dependence of the data of the extended RSRG. As noted in the last section, the extended RSRG can provide more accurate results as the number of kept states,  $m$ , increases. In the random AF case, the ground-state multiplet of a block Hamiltonian is either singlet or

doublet, depending on the number of original spins belonging to the block. The degeneracy of each low-lying excited multiplet is, therefore, always small. As a result, we can keep considerably many multiplets even if  $m$  is rather small. We estimate the  $m$ -dependence of the results of the extended RSRG from the numerical data with  $m = 10, 20, 30$ .

Figures 3 and 4 show, respectively, the numerical data of the mean correlations,  $\langle\langle C(r) \rangle\rangle$ , and the average of the logarithm of correlations,  $\langle\langle \ln C(r) \rangle\rangle$ , where  $\langle\langle \dots \rangle\rangle$  represents random average. It is clear that the data of the extended RSRG converge already at  $m = 30$ , and we can regard those data with  $m = 30$  as those in the limit  $m \rightarrow \infty$ . In Fig. 3 the data of the extended RSRG with  $m = 30$  are in good agreement with those of DMRG for  $r \lesssim 30$ , where the DMRG data are considered to be exact and free from finite-size effects. On the other hand, the conventional RSRG largely underestimates the correlations, but its data are on a line parallel to the data of the extended RSRG in the log-log plot. We conclude from these observations that the results of the extended RSRG are quantitatively reliable, whereas the conventional RSRG can be used to estimate the exponent of the power-law decay. Encouraged by the agreement between the extended RSRG and the DMRG data, we anticipate that the extended RSRG provide quantitatively reliable data even for  $r > 30$  where the reliable DMRG data are not available. From the data of the extended RSRG with  $m = 30$  for  $r \lesssim 300$ , where the data are expected not to be hampered by finite-size effects, we estimate the asymptotic form of the average correlations to be

$$\langle\langle C(r) \rangle\rangle \sim r^{-2}. \quad (15)$$

For the average of  $\ln C(r)$ , we also rely on the data obtained from the extended RSRG scheme. Figure 4 gives

$$\langle\langle \ln C(r) \rangle\rangle \sim -r^{0.5}. \quad (16)$$

Both results (15) and (16) agree with Fisher's theory<sup>2</sup> and can be considered as a numerical verification of his solution on the mean and typical correlations for the Heisenberg case. For the random  $XX$  chains<sup>18</sup> and for a related model of the random transverse-field Ising model,<sup>25</sup> the power-law behavior (15) and (16) is observed numerically. To our knowledge, Figs. 3 and 4 are first numerical results confirming Fisher's theory for the Heisenberg case.

## B. Random FM-AF case

Westerberg *et al.*<sup>19</sup> showed that the RG trajectories of the random FM-AF chains flow towards a single universal fixed point under the conventional RSRG procedure, unless the initial distribution of couplings is more singular than  $P(J_i) \sim |J_i|^{-y_c}$ ,  $y_c \sim 0.7$ . In this section we investigate the spin correlations at this fixed point with the extended RSRG scheme. For this purpose we assume the box-type bond distribution  $P(J_i)$ ,

$$P(J_i) = \begin{cases} \frac{1}{2J_0} & (-J_0 \leq J_i \leq J_0), \\ 0 & (\text{otherwise}), \end{cases} \quad (17)$$

with  $J_0$  as energy unit, as a representative of distributions with no singularity at  $J_i = 0$ . We expect that our results obtained for the initial distribution (17) should capture the universal behavior for the random FM-AF chains which are in the basin of the universal fixed point found in Ref. 19. We have numerically calculated spin correlations using the conventional RSRG, the extended RSRG with  $m = 30, 40, 50, 60$  and the DMRG method.

In the random FM-AF chains the degeneracy of the lowest multiplet of a block becomes larger on average as the size of the block grows. At the point when the degeneracy exceeds the number of kept states,  $m$ , determined beforehand in the algorithm, the extended RSRG scheme breaks down because we need to keep all the degenerate states in the lowest multiplet to preserve the  $SU(2)$  spin symmetry. In fact, we could complete the extended RSRG procedure without exceeding the limit of the number of kept states  $m = 30$  ( $m = 60$ ) for 30% (75%) of the sample chains ( $L = 1000$ ). We then used only those samples for which the RSRG could be completed to take the random average. Although this sorting out of sample chains may lead to a systematic underestimate on the average values, we believe that we can correct it by carefully checking the  $m$ -dependence of the data. The number of sample chains we used to take the random average for each RG scheme is shown in Table II.

The numerical results for the mean correlations,  $\langle\langle C(r) \rangle\rangle$ , are shown in Fig. 5 in a log-log plot. It is clear that the data of the extended RSRG have almost converged with  $m = 60$  for  $r < 500$ , where the data are expected to be free from the effect of the open boundaries. The data with  $m = 60$  are also in excellent agreement with the data of DMRG. We, therefore, regard the results of the mean correlation with  $m = 60$  as essentially converged. We notice that the curve in the log-log plot are bent upward, indicating that the mean correlations  $\langle\langle C(r) \rangle\rangle$  decay more slowly than a power-law. To analyze the  $r$ -dependence of the mean correlations, we plot the inverse of  $\langle\langle C(r) \rangle\rangle$  as a function of  $\ln r$  in the inset of Fig. 5. We find that the data lie on a straight line in this plot, from which we speculate that the mean correlations decay with the logarithmic form,

$$\langle\langle C(r) \rangle\rangle \sim \frac{a}{\ln(r/r_0)}, \quad (18)$$

where  $a$  and  $r_0$  are constants. We note, however, that Eq. (18) is not the only form that can account for the numerical data.<sup>26</sup> In any case the mean correlations show very weak  $r$ -dependence, probably through the form of  $\ln(r/r_0)$ , certainly different from power-law.

Figure 6 shows the numerical results of  $\langle\langle \ln C(r) \rangle\rangle$ . The data of the extended RSRG with  $m = 60$  exhibit a similar behavior to the logarithm of the mean correlations; The typical correlation  $\exp[\langle\langle \ln C(r) \rangle\rangle]$  decays again more slowly than a power-law. This leads us to plot the inverse of the typical correlations as a function of  $\ln r$  (see the inset of Fig. 6). Although the curve at  $m = 60$  seems almost linear for  $50 < r < 400$ , we cannot determine the  $r$ -dependence of the typical correlations from the figure due to the slow convergence of the data with increasing  $m$ . This slow convergence arises from the fact that the numerical estimate of  $\ln C(r)$  is very sensitive to small fluctuations of  $C(r)$  especially when the value of  $C(r)$  is extremely small. Calculations with much larger values of  $m$  would be needed to obtain the data accurate enough to determine the  $r$ -dependence of  $\langle\langle \ln C(r) \rangle\rangle$ .

### C. Distribution of the correlation functions

In order to make a distinction between characteristics of ground-state correlation functions in the random AF chains and in the random FM-AF chains, we analyze the distributions of the logarithm of the correlations,  $D(x; r)$ , where  $x = \ln C(r)$ . Henelius and Girvin<sup>18</sup> have shown numerically that for large  $r$  the distribution function of  $XX$  chains with random AF couplings scales to a fixed-point distribution of the form

$$D(x; r) = f(r)F(x/g(r)) \quad (19)$$

with

$$f(r)g(r) = 1, \quad (20)$$

$$g(r) = c |\langle\langle \ln C(r) \rangle\rangle|, \quad (21)$$

where  $c$  is a positive constant. The scaling function  $F(x/g(r))$  satisfies the normalization condition  $\int F(y)dy = 1$ . We will demonstrate that the distribution  $D(x; r)$  in random Heisenberg chains also exhibits the scaling behavior Eq. (19) for both the random AF and the random FM-AF case.

Figure 7 shows the data of  $D(x; r)$  for the random AF case obtained using the extended RSRG with  $m = 30$ . According to Eqs. (16) and (21), we can set  $g(r) = r^{0.5}$  and  $f(r) = r^{-0.5}$ . The data points (circles and squares) in Fig. 7 collapse on a single curve, indicating that the scaling (19) applies.<sup>27</sup> In Fig. 7 we also plot

$$W(x; r) = \frac{e^x D(x; r)}{\langle\langle C(r) \rangle\rangle}, \quad (22)$$

which measures the contribution to the mean value of the correlation  $\langle\langle C(r) \rangle\rangle$ . Although the curves are rather rough due to a statistical error, it is clear that  $W(x; r)$  has a considerable weight in the range where  $D(x; r)$  is very small. This means that a very few spin pairs that have much stronger correlations than typical ones give dominant contribution to the mean correlation  $\langle\langle C(r) \rangle\rangle$ . We also find that, as  $r$  increases, the region of  $x/g(r)$  where  $W(x; r)$  is large moves towards  $x/g(r) = 0$ . Indeed this is the behavior expected from Eq. (15); the value of  $x/g(r)$  where  $W(x; r)$  takes a large weight should change as  $\ln \langle\langle C(r) \rangle\rangle / g(r) \sim \ln r / r^{0.5} \rightarrow 0$  as  $r \rightarrow \infty$ . Thus we regard the results shown in Fig. 7 as a further support for the random-singlet picture of the ground state of the random AF Heisenberg chains, where each spin forms a singlet pair with another spin that can be arbitrarily far away. The mean correlation  $\langle\langle C(r) \rangle\rangle$  is dominated by the contribution from the rare case in which two spins separated by distance  $r$  form a spin singlet.

Figure 8 shows the numerical data of  $D(x; r)$  of the extended RSRG with  $m = 60$  for the random FM-AF chains. Here we set  $g(r) = \langle\langle \ln C(r) \rangle\rangle / \langle\langle \ln C(r = 200) \rangle\rangle$  and  $f(r) = 1/g(r)$ . The data points (circles and squares) for  $100 < r < 500$ , where we may ignore the boundary effect, clearly lie on a single scaling curve. In this range of  $r$ , however,  $g(r)$  changes by several percent only, from 0.95 to 1.04. To establish the scaling behavior for wide range of  $g(r)$ , the calculations on much (exponentially) larger systems might be necessary. Such large-scale calculations are obviously unfeasible with computers available at present, and thus we can only conclude that our results shown in Fig. 8 are consistent with the scaling hypothesis (19). In the following discussion, we regard  $D(x; r)/f(r)$  in Fig. 8 as a fixed-point form of the distribution function.

Figure 8 clearly shows that the distribution function of the random FM-AF chains has a quite different form from that of the random AF chains. It is essentially zero for  $x/g(r) \gtrsim -1$  and increases approximately linearly at  $x/g(r) \lesssim -1$ . The weight function  $W(x; r)$  representing the contribution to the mean correlation is also shown in Fig. 8. In contrast to the random AF case,  $W(x; r)$  has most of its weight in the region where  $D(x; r)$  is not negligible. This feature highlights the different nature of the spin correlations in the random FM-AF chains. As shown in the RSRG analysis, many spins in the random FM-AF chains correlate and form a large effective spin. This suggests that a spin is correlated with many other spins that belong to the same large effective spin, and, therefore, the mean value of the spin correlation function is not at all dominated by the “rare” events that two spins, far apart from each other, form a singlet pair.

From the observation that  $D(x; r)/f(r)$  of the random FM-AF chains is negligible for  $x/g(r) > -A$  ( $A \approx 1$  in Fig. 8) and has an approximately linear dependence for  $x/g(r) < -A$  until it takes a maximum value, we can also draw a conclusion that  $\ln\langle\langle C(r)\rangle\rangle$  and  $\langle\langle \ln C(r)\rangle\rangle$  should have a similar dependence on  $r$ , in agreement with Figs. 5 and 6. Let us assume that the scaling function has the form

$$F(y) = \begin{cases} -k(y + A) & y \leq -A, \\ 0 & y > -A, \end{cases} \quad (23)$$

where  $y = x/g(r)$ ,  $k$  and  $A$  are positive constants. Since  $g(r) \rightarrow \infty$  in the limit  $r \rightarrow \infty$ , the mean correlation  $\langle\langle C(r)\rangle\rangle$  is dominated by the contribution from the region of small  $|x/g(r)|$ . Thus, we are allowed to use Eq. (23) for calculating  $\langle\langle C(r)\rangle\rangle$ , even though this form is not correct for large  $|x/g(r)|$ . Using Eqs. (19), (20) and (23), we calculate the mean correlation:

$$\langle\langle C(r)\rangle\rangle = \int e^x D(x; r) dx = -k \int_{-\infty}^{-Ag(r)} e^x \left( \frac{x}{g(r)} + A \right) dx = \frac{k}{[g(r)]^2} e^{-Ag(r)},$$

yielding

$$\ln\langle\langle C(r)\rangle\rangle = -Ag(r) + \mathcal{O}(\ln g(r)) = Ac\langle\langle \ln C(r)\rangle\rangle + \mathcal{O}(\ln |\langle\langle \ln C(r)\rangle\rangle|) \quad (24)$$

in the limit  $r \rightarrow \infty$ . This result is in agreement with our observation that the curves in Figs. 5 and 6 look very similar. It is also consistent with the fact that  $W(x; r)$  in Fig. 8 stays almost in the same region of  $x/g(r)$  with increasing  $r$ . Equation (24) is not changed qualitatively even when  $F(y)$  has an algebraic form  $F(y) \propto [-(y + A)]^\alpha$ , as far as  $A > 0$ . Note that Eq. (24) does not hold in the random AF chains, for which we should take  $A = 0$  and  $\alpha = 3$ .

#### IV. CONCLUSION

We have studied the spin correlations in spin- $\frac{1}{2}$  random Heisenberg chains for both the random AF and the random FM-AF case. One of the most powerful methods for the study of random spin chains is the real-space RG in which the spin degrees of freedom are decimated by integrating out the strongest bonds successively. In order to calculate the two-spin correlation functions between original  $S = \frac{1}{2}$  spins, we modified the algorithm of the conventional RSRG using the Wigner-Eckart theorem. We also extended the RSRG scheme by keeping the local excited multiplets as block states to keep track of quantum effects. We demonstrated that the extended RSRG algorithm is very powerful, in the sense that it can be applied to rather large systems, and provides accurate numerical data that are in excellent agreement with those of the DMRG method. The numerical data of the mean and typical correlations for the random AF chains verified Fisher’s prediction [Eqs. (15) and (16)] for the Heisenberg case, which cannot be mapped to noninteracting fermions. For the random FM-AF chains, we found that the mean correlation,  $\langle\langle C(r)\rangle\rangle$ , decays very slowly with the logarithmic  $r$ -dependence. We, therefore, conclude that the generalized staggered spin correlation in the random FM-AF chains has no LRO, although it shows very long-range correlations decaying slower than power-law behavior. Investigating the distribution of the logarithm of the spin correlation functions, we also clarified the different nature of the ground states of the random AF and FM-AF chains. In both cases, our data of distributions satisfy the scaling hypothesis, Eq. (19). Analyzing the form of the scaling function, we found that the “rare spin pairs”, which are correlated much stronger than typical ones, dominate the mean correlation  $\langle\langle C(r)\rangle\rangle$  in the random AF case. It is also shown that the  $r$ -dependence of the mean correlations in this case is quite different from that of the typical ones. These features strongly support the fact that the “random singlet phase” is realized in the ground state of the random AF Heisenberg chains. On the other hand, the scaling form of the distribution functions for the random FM-AF chains suggests that such “rare spin pairs” do not play an important role in these chains. We also deduced that  $\ln\langle\langle C(r)\rangle\rangle$  and  $\langle\langle \ln C(r)\rangle\rangle$  have very similar  $r$ -dependence, using the scaling hypothesis and the specific feature of the scaling function we obtained numerically. This result is non-trivial and consistent with our numerical data (Figs. 5 and 6).



## ACKNOWLEDGMENTS

HT was supported by the Research Fellowship of the Japan Society for the Promotion of Science for Young Scientists. The work of AF and MS was in part supported by a Grant-in-Aid from the Ministry of Science, Education and Culture of Japan. Numerical calculations were carried out at the Yukawa Institute Computing Facility.

- <sup>1</sup> S.-k. Ma, C. Dasgupta, and C.-k. Hu, Phys. Rev. Lett. **43**, 1434 (1979); C. Dasgupta and S.-k. Ma, Phys. Rev. B **22**, 1305 (1980).
- <sup>2</sup> D. S. Fisher, Phys. Rev. B **50**, 3799 (1994).
- <sup>3</sup> R. A. Hyman, Kun Yang, R. N. Bhatt, and S. M. Girvin, Phys. Rev. Lett. **76**, 839 (1996); R. A. Hyman and Kun Yang, Phys. Rev. Lett. **78**, 1783 (1997); Kun Yang and R. N. Bhatt, Phys. Rev. Lett. **80**, 4562 (1998).
- <sup>4</sup> M. Fabrizio and R. Mélin, Phys. Rev. Lett. **78**, 3382 (1997).
- <sup>5</sup> C. Monthus, O. Golinelli, and Th. Jolicoeur, Phys. Rev. Lett. **79**, 3254 (1997).
- <sup>6</sup> L. N. Bulaevskii, A. V. Zvarykina, Yu. S. Karimov, R. B. Lyubovskii, and I. F. Shchegolev, Zh. Eksp. Teor. Fiz. **62**, 725 (1972) [Sov. Phys. JETP **35**, 384 (1972)]; L. J. Azevedo and W. G. Clark, Phys. Rev. B **16**, 3252 (1977).
- <sup>7</sup> G. Theodorou and M. H. Cohen, Phys. Rev. Lett. **37**, 1014 (1976); G. Theodorou, Phys. Rev. B **16**, 2264, 2273 (1977).
- <sup>8</sup> T. N. Nguyen, P. A. Lee, and H.-C. zur Loye, Science **271**, 489 (1996).
- <sup>9</sup> A. Furusaki, M. Sigrist, P. A. Lee, K. Tanaka, and N. Nagaosa, Phys. Rev. Lett. **73**, 2622 (1994); A. Furusaki, M. Sigrist, E. Westerberg, P. A. Lee, K. B. Tanaka, and N. Nagaosa, Phys. Rev. B **52**, 15930 (1995).
- <sup>10</sup> M. Azuma, Y. Fujishiro, M. Takano, M. Nohara, and H. Takagi, Phys. Rev. B **55**, R8658 (1997); M. Azuma, M. Takano, and R. S. Eccleston, J. Phys. Soc. Jpn. **67**, 740 (1998).
- <sup>11</sup> Y. Motome, N. Katoh, N. Furukawa, and M. Imada, J. Phys. Soc. Jpn. **65**, 1949 (1996); Y. Iino and M. Imada, J. Phys. Soc. Jpn. **65**, 3728 (1996).
- <sup>12</sup> H. Fukuyama, N. Nagaosa, M. Saito, and T. Tanimoto, J. Phys. Soc. Jpn. **65**, 2377 (1996).
- <sup>13</sup> M. Sigrist and A. Furusaki, J. Phys. Soc. Jpn. **65**, 2385 (1996); N. Nagaosa, A. Furusaki, M. Sigrist, and H. Fukuyama, J. Phys. Soc. Jpn. **65**, 3724 (1996).
- <sup>14</sup> G. B. Martins, E. Dagotto, and J. A. Riera, Phys. Rev. B **54**, 16032 (1996).
- <sup>15</sup> H.-J. Mikeska, U. Neugebauer, and U. Schollwöck, Phys. Rev. B **55**, 2955 (1997).
- <sup>16</sup> T. Miyazaki, M. Troyer, M. Ogata, K. Ueda, and D. Yoshioka, J. Phys. Soc. Jpn. **66**, 2580 (1997).
- <sup>17</sup> M. Greven and R. J. Birgeneau, Phys. Rev. Lett. **81**, 1945 (1998).
- <sup>18</sup> P. Henelius and S. M. Girvin, Phys. Rev. B **57**, 11457 (1998).
- <sup>19</sup> E. Westerberg, A. Furusaki, M. Sigrist, and P. A. Lee, Phys. Rev. Lett. **75**, 4302 (1995); Phys. Rev. B **55**, 12578 (1997).
- <sup>20</sup> B. Frischmuth and M. Sigrist, Phys. Rev. Lett. **79**, 147 (1997); B. Frischmuth, M. Troyer, B. Ammon, and M. Sigrist, cond-mat/9808027.
- <sup>21</sup> See, for example, J. J. Sakurai, *Modern Quantum Mechanics* (Benjamin/Cummings, Menlo Park, 1985) p.238.
- <sup>22</sup> S. R. White, Phys. Rev. Lett. **69**, 2863 (1992); Phys. Rev. B **48**, 10345 (1993).
- <sup>23</sup> S. R. White, Phys. Rev. Lett. **77**, 3633 (1996).
- <sup>24</sup> K. Hida, J. Phys. Soc. Jpn. **66**, 330 (1997).
- <sup>25</sup> A. P. Young and H. Rieger, Phys. Rev. B **53**, 8486 (1996).
- <sup>26</sup> We also tried the stretched exponential form,  $\exp\{-\tilde{a}[\ln(r/\tilde{r}_0)]^\gamma\}$ , with which we could fit the numerical data as well as with Eq. (18). Here  $\tilde{a}$ ,  $\tilde{r}_0$ , and  $\gamma$  are constants.
- <sup>27</sup> Some data points at  $x/g(r) < -1$  are off the scaling curve in Fig. 7. We estimate that the numerical error in  $C(r)$  in our calculation is of order  $10^{-8}$ . The scattered data are those with small correlations of order  $10^{-7}$ . Thus the failure of the data collapse at  $x/g(r) < -1$  does not mean the violation of the scaling.

RG scheme	number of samples
conventional RSRG	200
extended RSRG ( $m = 10$ )	2460
extended RSRG ( $m = 20$ )	1878
extended RSRG ( $m = 30$ )	1899
DMRG	1887

TABLE I. The number of samples simulated to take the random averages in the random AF chains.

RG scheme	number of samples
conventional RSRG	150
extended RSRG ( $m = 30$ )	1319
extended RSRG ( $m = 40$ )	1446
extended RSRG ( $m = 50$ )	1890
extended RSRG ( $m = 60$ )	1557
DMRG	204

TABLE II. The number of samples simulated to take the random averages in the random FM-AF chains.

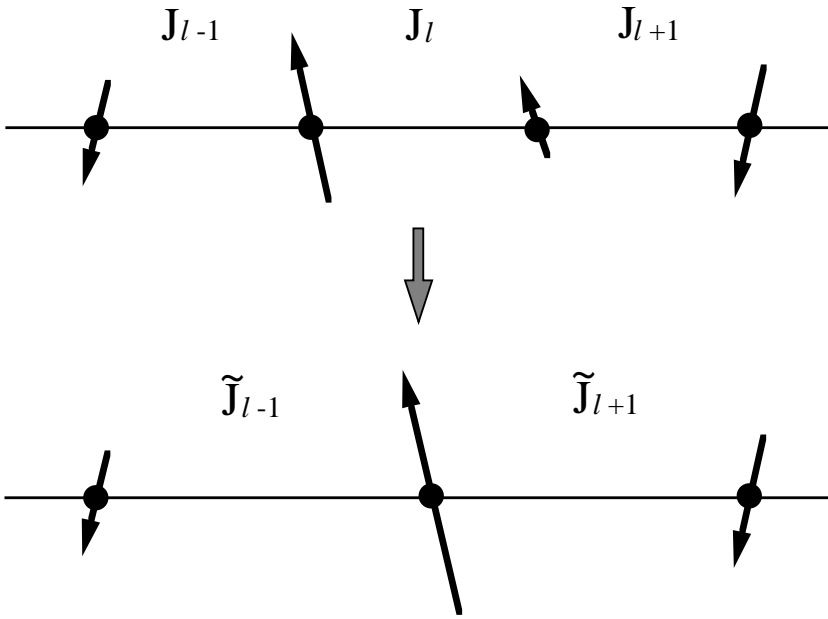


FIG. 1. Schematic picture of renormalization procedure in the conventional RSRG.

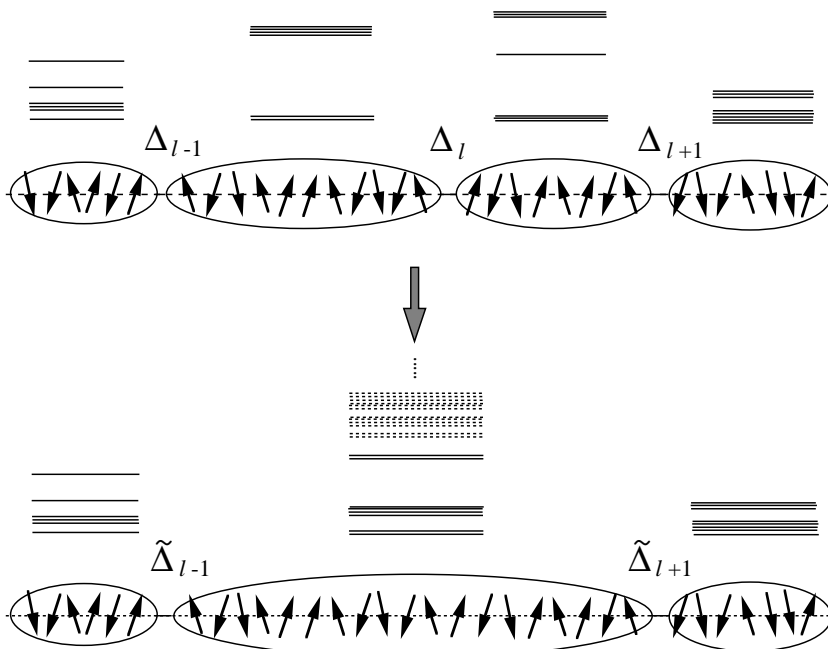


FIG. 2. Schematic picture of renormalization procedure in the extended RSRG. The dashed and solid lines represent eigenstates of each block Hamiltonian which are discarded and kept, respectively.

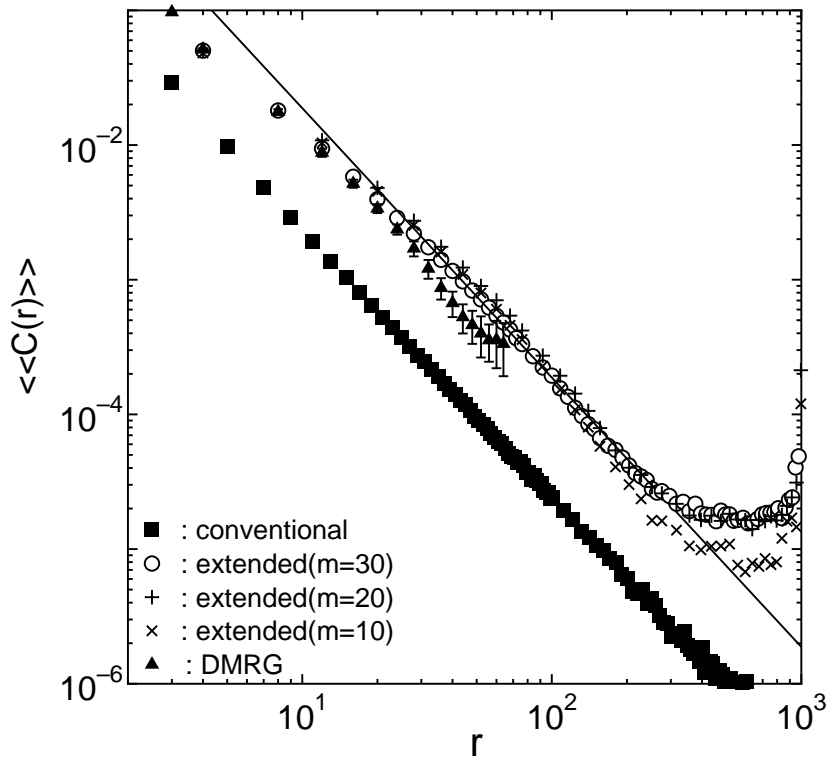


FIG. 3. The mean correlation  $\langle\langle C(r) \rangle\rangle$  of random AF chains as a function of  $r$ . The solid line corresponds to the  $r^{-2}$  decay. The statistical errors of the data of the extended RSRG for  $r < 300$  and of the conventional RSRG is smaller than the size of symbols.

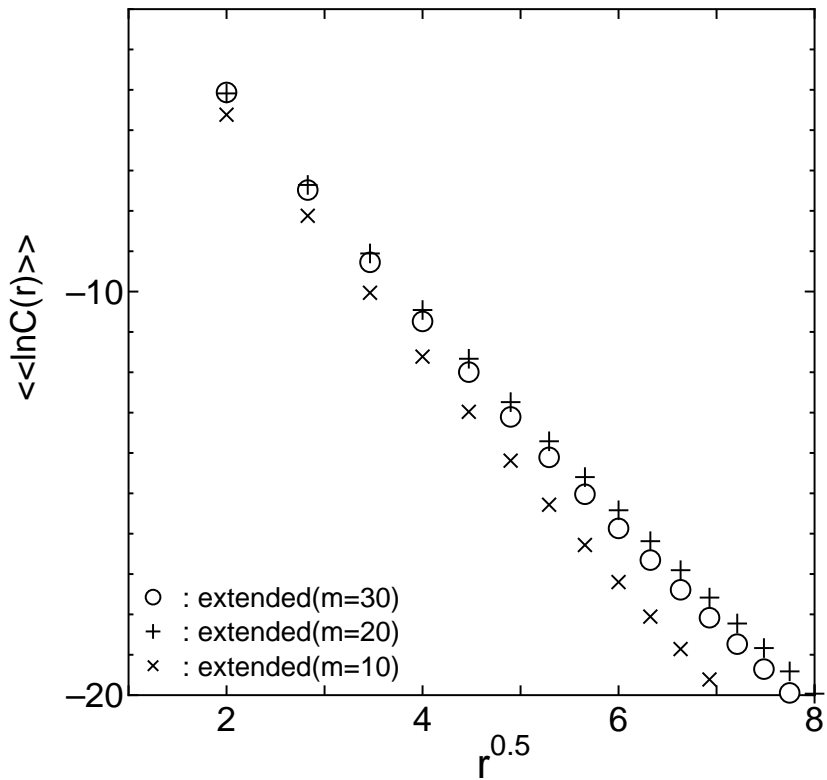


FIG. 4.  $\langle\langle \ln C(r) \rangle\rangle$  versus  $r^{0.5}$  for the random AF case. The statistical errors of the data are smaller than the size of symbols.

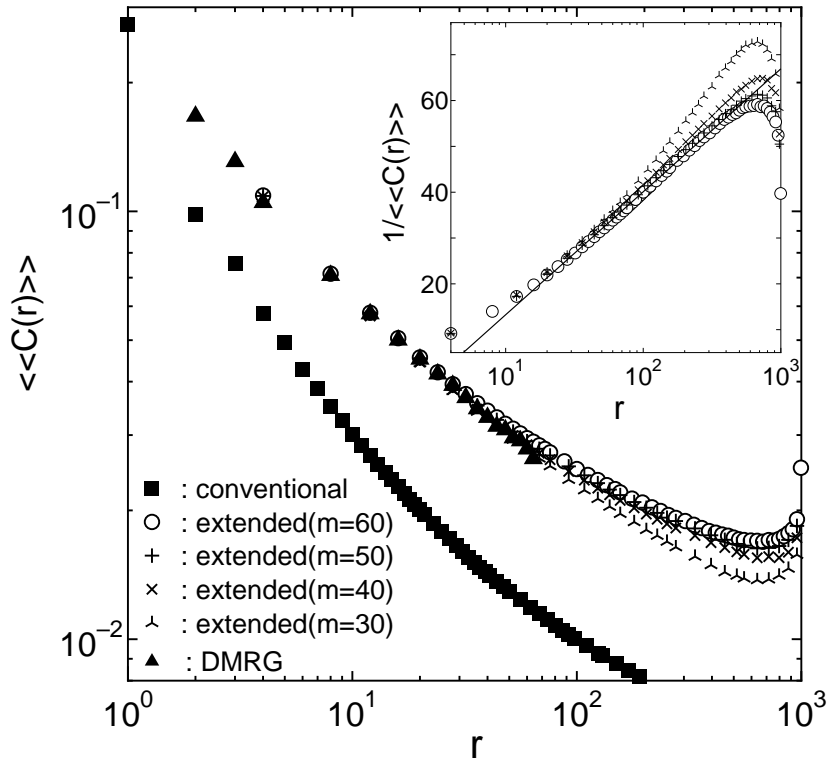


FIG. 5.  $\langle\langle C(r) \rangle\rangle$  of random FM-AF chains as a function of  $r$ . The statistical errors of the data are smaller than the size of symbols. Inset:  $1/\langle\langle C(r) \rangle\rangle$  versus  $r$ .

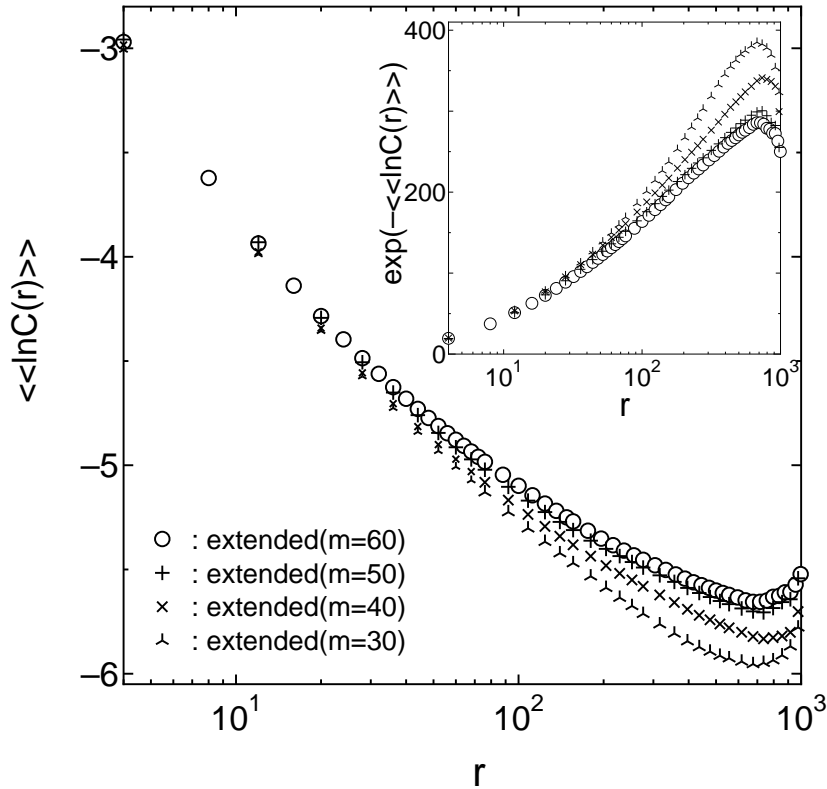


FIG. 6.  $\langle\langle \ln C(r) \rangle\rangle$  of the random FM-AF case as a function of  $r$ . The statistical errors of the data for  $r < 500$  are smaller than the size of symbols. Inset:  $\exp[-\langle\langle \ln C(r) \rangle\rangle]$  versus  $r$ .

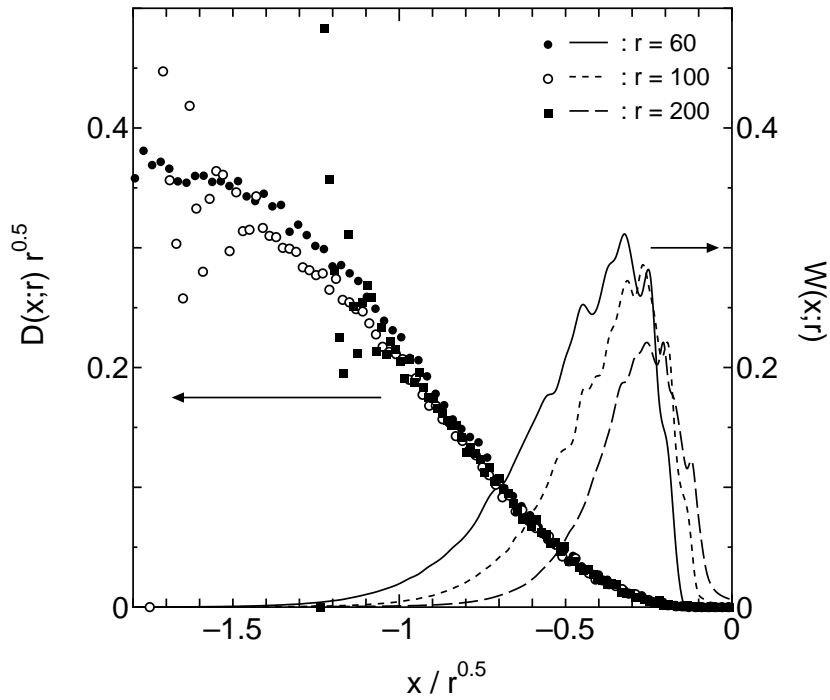


FIG. 7. Probability distributions of the correlation functions in the random AF case for  $r = 60, 100, 200$ .  $W(x; r)$  is also plotted for  $r = 60, 100, 200$  with a solid, dotted, dashed curve, respectively.

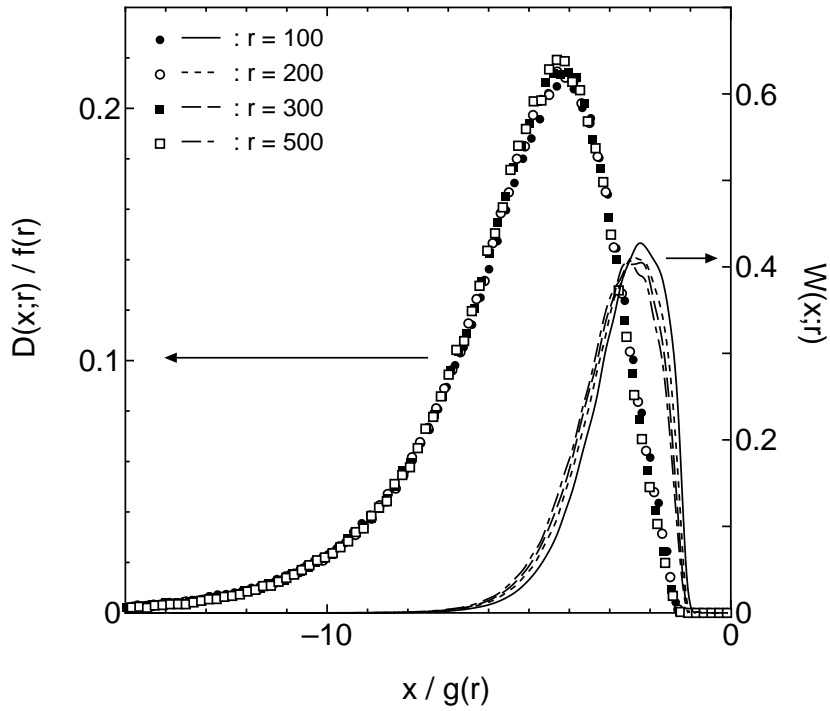


FIG. 8. Probability distributions of the correlation functions in the random FM-AF case for  $r = 100, 200, 300, 500$ .  $W(x; r)$  is also plotted for  $r = 100, 200, 300, 500$  with a solid, dotted, dashed, dot-dashed curve, respectively.